Cell Death and Differentiation (2014), 1–10

www.nature.com/cdd

Loss of *Prkar1a* leads to Bcl-2 family protein induction and cachexia in mice

L Gangoda[1], M Doerflinger[1], R Srivastava[1], N Narayan[2], LE Edgington[1], J Orian[1], C Hawkins[1], LA O'Reilly[2,3], H Gu[4], M Bogyo[5], P Ekert[2], A Strasser[2,3] and H Puthalakath*[,1]

Loss of function mutations in the *Prkar1a* gene are the cause of most cases of Carney complex disorder. Defects in *Prkar1a* are thought to cause hyper-activation of PKA signalling, which drives neoplastic transformation, and *Prkar1a* is therefore considered to be a tumour suppressor. Here we show that loss of *Prkar1a* in genetically modified mice caused transcriptional activation of several proapoptotic *Bcl-2* family members and thereby caused cell death. Interestingly, combined loss of *Bim* and *Prkar1a* increased colony formation of fibroblasts in culture and promoted their growth as tumours in immune-deficient mice. Apart from inducing apoptosis, systemic deletion of *Prkar1a* caused cachexia with muscle loss, macrophage activation and increased lipolysis as well as serum triglyceride levels. Loss of single allele of *Prkar1a* did not enhance tumour development in a skin cancer model, but surprisingly, when combined with the loss of *Bim*, caused a significant delay in tumorigenesis and this was associated with upregulation of other BH3-only proteins, PUMA and NOXA. These results show that loss of *Prkar1a* can only promote tumorigenesis when *Prkar1a*-mediated apoptosis is somehow countered.
Cell Death and Differentiation advance online publication, 11 July 2014; doi:10.1038/cdd.2014.98

Carney complex (CNC), a rare disorder with fewer than 750 affected individuals identified worldwide since 1985, is an inheritable autosomal dominant condition characterized by spotty skin pigmentation (lentiginosis and epithelioid blue naevus), cardiac and other myxomas, endocrine tumours (Cushing syndrome) and psammomatous melanotic schwannomas.[1] CNC patients have substantially decreased life-span with ~60% of deaths due to heart-related morbidities and the remainder due to post-operative complications or malignant disease.[2] Carney complex disease shares similarities with the McCune–Albright syndrome (MAS), particularly paradoxical responses to endocrine signals; accordingly, mutations of genes involved in cyclic nucleotide (e.g., cAMP, cGMP) mediated signalling are implicated in both syndromes.[3]

Notably, two thirds of patients with Carney complex syndrome have heterozygous mutations in the *Prkar1a* gene (chromosome 17q24), which encodes the regulatory subunit RIα (PRKAR1α) of cAMP-dependent protein kinase A (PKA). PRKAR1α protein insufficiency leads to lack of regulation with consequent overactivation of the PKA signalling pathway. More than 117 mutations in the *Prkar1a* gene have been found to cause Carney complex. Most of these mutations result in premature stop codons leading to a complete loss of the PRKAR1α protein.[4] There are also descriptions of CNC cases in which splice site mutations cause exon 6 skipping with consequent expression of an abnormally shortened PRKAR1α protein that can be detected in leukocytes and tumours. These data suggest that haploinsufficiency, not only its complete loss, can cause abnormally increased PKA activity leading to tumorigenesis in CNC patients.[5] How the loss or deficiency in PRKAR1α causes tumour development in CNC remains unclear. Haploinsufficiency of *Prkar1a* with consequent imbalance in the ratio between PRKAR1α to PRKARIIβ (R2beta regulatory subunit of PKA) was proposed to cause tumour development in some cases.[6] Increased PKA activity increases extracellular receptor kinase (ERK1/2) mitogen-activated protein kinase (MAPK) pathway signalling.[7,8] This causes an increase in the levels of the transcription factors c-MYC and c-FOS. Notably, PRKAR1α deficiency also promotes activation of cyclin D1, Cdk4 and E2F1, which all drive cell cycle progression.[9,10]

Although increased PKA activity was shown to enhance cellular proliferation, there is also emerging evidence that it can also restrain cell growth, for example, by promoting apoptotic cell death. Findings from our laboratory and others revealed that increased PKA activity caused transcriptional induction as well as posttranslational stabilization of the proapoptotic BH3-only protein BIM.[11–13] Moreover, PKA activation has been shown to promote differentiation and block proliferation in certain cell lines.[14–17] Increased PKA activity has also been reported to cause cardiomyocyte apoptosis, thereby leading to cardiomyopathy.[18] It has been proposed that PKA agonists may be useful agents for the treatment of leukaemia,[19] based on the notion that increased PKA activity can trigger apoptosis. Therefore, *Prkar1a* mutation driven cancers would be expected to develop only if they sustained additional mutations or epigenetic changes (e.g., those that cause a reduction in *Bim* levels)

[1]Department of Biochemistry, La Trobe Institute of Molecular Science, La Trobe University, Melbourne, Victoria, Australia; [2]The Walter and Eliza Hall Institute, Melbourne, Victoria, Australia; [3]Department of Medical Biology, University of Melbourne, Melbourne, Victoria, Australia; [4]Institut de Recherches Cliniques de Montréal (IRCM) Department of Microbiology and Immunology, University of Montreal and Division of Experimental Medicine, McGill University Montreal, Montreal, Quebec, Canada and [5]Cancer Biology Program, Department of Pathology, Stanford School of Medicine, Stanford, CA, USA
*Corresponding author: H Puthalakath, Department of Biochemistry, La Trobe University, Melbourne, Victoria 3086, Australia. Tel: +61 3 94795226; Fax: +61 3 94791266; E-mail: h.puthalakath@latrobe.edu.au
Abbreviations: cAMP-PKA, Cyclic-AMP regulated protein kinase A; 4-OHT, 4-Hydroxytamoxifen; PKA regulatory subunit 1a; CNC, Carney complex
Received 11.12.13; revised 07.6.14; accepted 10.6.14; Edited by RA Knight

that inhibit apoptosis. In the present study, we tested this hypothesis by investigating the functional interactions between *Bim* and loss of *Prkar1a* on tumorigenesis, using both allograft as well as orthotopic mouse models. Our data show that loss of *Prkar1a* leads to apoptosis in diverse cell types and cachexia and that this is associated with upregulation of several proapoptotic BCL-2 family members. This indicates that tumorigenesis driven by mutations in *Prkar1a* require acquisition of abnormalities that block apoptosis.

Results

Prkar1a deletion resulted in increased Bim expression, increased apoptosis and reduced clonogenic survival in MEFs. Conventional Cre recombinase-mediated deletion of 'floxed' *Prkar1a* alleles caused widespread attenuation of the PKA signal pathway in many tissues. This was observed with lentivirally or retrovirally introduced CRE as well as tissue specifically expressed *Cre* transgenes, such as the T cell-specific *LCK-Cre* or the B cell-specific *CD19-Cre* transgenes.[20] However, use of an inducible Cre recombinase (CRE-ER^{T2}, a fusion protein of CRE with the oestrogen receptor) could circumvent this problem.[20] This recombinase is latent because it is sequestered in the cytoplasm by HSP90. Addition of tamoxifen causes release of CRE-ER^{T2} from HSP90, allowing it to enter the nucleus where it will recombine floxed target genes, such as *Prkar1a* in our study. We intercrossed *ROSA-CreER^{T2}* (B6.129-*Gt(ROSA)26-Sortm1(cre/ERT2)Tyj*/J) mice[21] with *Bim*$^{-/-}$ and *Prkar1a*$^{fl/fl}$ mice to obtain MEFs of the following genotypes: *ROSA-CreER*$^{tg/tg}$*;wt, ROSA-CreE*$^{tg/tg}$*;Prkar1a*$^{fl/fl}$ *and ROSA-CreER*$^{tg/tg}$*;Prkar1a*$^{fl/fl}$*;Bim*$^{-/-}$ all bearing the *ROSA-CreER^{T2}* transgene. Treating the *ROSA-*^{CreERT2}*;Prkar1a*$^{fl/fl}$ MEFs with 2 μM 4-hydroxytamoxifen (4-OHT) led to near complete loss of Prkar1α protein within 72 h (Figure 1a). Quantitative PCR (qPCR) confirmed efficient deletion of the *Prkar1a* '*floxed*' alleles (Figure 1b). The qPCR analysis also showed that *Nur77,* a firmly established downstream transcriptional target of PKA, was upregulated upon *Prkar1a* deletion (Figure 1b). Recovery of cells from 4-OHT was not necessary as seen by the p-PKA substrate levels in the western blot (Figure 1a). There was also a marked increase

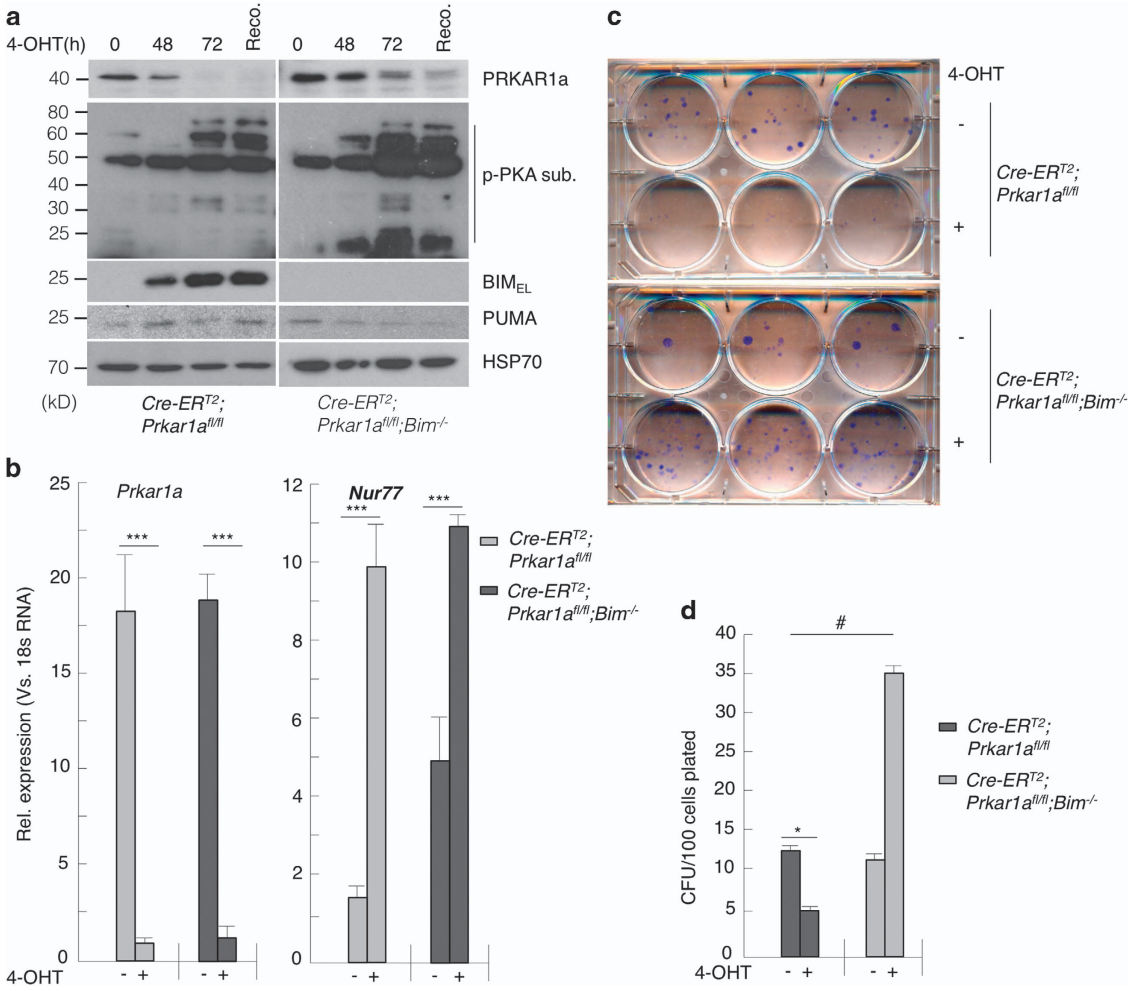

Figure 1 CRE-ER^{T2}-mediated deletion of *Prkar1a* caused an increase in PKA activation and apoptosis in MEFs. (**a**) Western blot and (**b**) qPCR analyses to determine the impact of *Prkar1a* deletion on PKA activation and expression of *Bim*. p-PKA-sub is a substrate of PKA. *Nur77* is a gene that is activated by PKA. (**c** and **d**) Clonogenic survival of MEFs after *Prkar1a* deletion. Error bars ± S.E.M., $n = 3$, two-tailed *t*-tests. ***$P = 1.2^{E-4}$; *$P = 0.02$, $^{\#}P = 0.0016$

in BIM protein and *Bim* mRNA levels (Figure 1a and Supplementary Figure S1a), but we failed to see a significant induction of PUMA protein or *Puma* mRNA in these MEFs (Figure 1a and Supplementary Figure S1b). This was not due to the loss of p53 function because of the expression of SV40 T-antigen that was used to immortalize these cells as primary MEFs (with p53 function) also failed to show *Puma* upregulation in response to *Prkar1a* deletion (data not shown). Interestingly, inducible loss of *Prkar1a* in MEFs caused a significant reduction in their clonogenic survival, but this could be rescued completely by constitutive loss of *Bim* (Figures 1c and d). Indeed in the absence of *Bim*, increased PKA activity (caused by deletion of *Prkar1a*) augmented colony formation of MEFs significantly above that seen for control MEFs (i.e. no deletion of *Prkar1a* and no loss of *Bim*; Figures 1c and d). We also observed a change in Bim phosphorylation in *Prkar1a*-deleted MEFs, which could be reversed by the PKA inhibitor H-89 (Supplementary Figure S1c). However, the contribution of Bim protein stabilization[11] to apoptosis in these MEFs is yet to be determined.

Collectively, these data show that inducible deletion of *Prkar1a* triggers apoptosis and consequently reduced colony formation in MEFs by causing an upregulation of *Bim* expression.

Combined loss of Prkar1a and Bim promoted tumour growth by MEFs in immune-deficient mice. PRKAR1α deficiency is known to increase the expression of cyclin D1, Cdk4 and E2F1, which all promote cell cycle progression.[9] We hypothesized that this tumour-promoting activity of *Prkar1a* loss is countered by its ability to also increase the propensity of cells to undergo apoptosis (due to induction of *Bim*). Since *Bim*$^{-/-}$ - *Prkar1a* $^{-/-}$ MEFs formed significantly more colonies in culture compared with *Prkar1a* $^{-/-}$ MEFs, we wondered whether loss of *Prkar1a* and loss of *Bim* could cooperate to promote tumour development *in vivo*. We examined this by injecting immunodeficient athymic nude mice subcutaneously (s.c.) with *Wt*, *Prkar1a* $^{fl/fl}$, *Prkar1a* $^{-/-}$, *Bim*$^{-/-}$; *Prkar1a* $^{fl/fl}$ or *Bim*$^{-/-}$;*Prkar1a* $^{-/-}$ MEFs. Although MEFs in which *Prkar1a* had been deleted failed to form tumours in nude mice, combined loss of *Prkar1a* and *Bim* rapidly caused readily detectable subcutaneous tumours in 100% recipients (750 mm^3 in approximately four weeks when the mice had to be culled according to ethics guidelines; Figures 2a and b). As additional controls, none of the nude mice injected with *Wt*, *Prkar1a*$^{fl/fl}$ or *Bim*$^{-/-}$ MEFs developed tumours. This demonstrates that cells must lose both PRKAR1α and BIM to be able to grow as tumours *in vivo*. Interestingly, cells from the tumours formed by *Bim*$^{-/-}$; *Prkar1a*$^{-/-}$ MEFs exhibited increased H2AX phosphorylation (γ-H2AX staining) compared with the same cells maintained in culture (Figures 2c and d). This indicates that these cells may exhibit genomic instability *in vivo*, which may drive their oncogenic transformation.[22,23] Collectively, these results demonstrate that loss of *Prkar1a* cooperates with loss of *Bim* in tumour development, at least in MEFs.

Prkar1a deletion leads to PKA activation, increased Bim and Puma expression and consequent apoptosis in several mouse tissues. Next, we examined the consequences of loss of *Prkar1a* in non-transformed cells within the whole animal. Loss of *Prkar1a* in all cells from conception causes embryonic lethality.[24] We therefore intercrossed *Prkar1a* $^{fl/fl}$ and *Bim*$^{-/-}$;*Prkar1a*$^{fl/fl}$ mice with *ROSA-CreER*^{T2} transgenic mice to generate *ROSA-CreERT2;Prkar1a*$^{fl/+}$, *ROSA-CreER*^{T2}*;Prkar1a*$^{fl/fl}$, *ROSA-CreER*^{T2}*;Bim*$^{-/-}$*;Prkar1a*$^{fl/+}$ and *ROSA-CreER*^{T2};*Prkar1a*$^{fl/fl}$; *Bim*$^{-/-}$ mice. In the *ROSA-CreER*^{T2}*;Prkar1a*$^{fl/+}$ and *ROSA-CreER*^{T2}*;Prkar1a*$^{fl/fl}$ mice, a single intraperitoneal (i.p.) injection of tamoxifen (40 mg/kg) was sufficient to achieve near complete deletion of the '*floxed*' *Prkar1a* alleles, as verified by qPCR and digital PCR analyses (Figure 3a and Supplementary Figure S2). Deletion of either one or both *Prkar1a* alleles resulted in increased PKA activation as demonstrated by increased phospho-PKA substrate levels in various tissues, including heart, liver, lung and spleen (Figures 3b and c). This was accompanied by increases in the proapoptotic BH3-only proteins BIM and PUMA (Figures 3b and c). The largest increase in BIM levels was observed in the liver, presumably due to the fact that this is the site of tamoxifen metabolism and hence *Prkar1a*$^{fl/fl}$ alleles are deleted most efficiently. In the spleen, there was only a minor increase in BIM_{EL} levels but a marked increase in the smaller isoforms BIM_L and BIM_S (Figures 3b and c). In *ROSA-CreER*^{T2}*;Prkar1a*$^{fl/fl}$*;Bim* $^{-/-}$ mice, induced deletion of *Prkar1a* caused a marked increase in the levels of PUMA as seen by the western blot analysis, whereas, as expected, BIM was not detectable (Figures 3b and c, second panel). The reason for this increased upregulation of PUMA is not understood but it is possible that the loss of BIM allows the cells to cope with increased amounts of PUMA elicited by induced *Prkar1a* deletion.

TUNEL staining showed significant increases in apoptosis in several tissues from tamoxifen-injected *ROSA-CreER*^{T2}*;Prkar1a*$^{fl/fl}$ mice compared with tissues from control animals (Figures 4a and b). This cell death was significantly, albeit not completely, reduced by loss of *Bim* (in tamoxifen-injected *ROSA-CreER*^{T2}*; Prkar1a* $^{fl/fl}$*;Bim* $^{-/-}$ mice). Although loss of *Bim* could almost completely abrogate *Prkar1a* deletion-induced cell death in the spleen and liver, other tissues such as kidney and heart from tamoxifen-injected *ROSA-CreERT2;Prkar1a*$^{fl/fl}$*;Bim*$^{-/-}$ mice still contained significantly more dying cells compared with control animals (Figure 4b). This can probably be attributed to the substantial increase in *Puma* levels observed in these tissues after *Prkar1a* deletion (Figure 3).

Prkar1a deletion causes weight loss and cachexia in mice. Administration of tamoxifen at 40 mg/kg body weight for three consecutive days to *ROSA-CreERT2;Prkar1a*$^{fl/fl}$ and even *ROSA-CreER*^{T2}*;Prkar1a*$^{fl/fl}$*;Bim* $^{-/-}$ mice led to rapid weight loss and death on the fourth day. Injection of a single dose of tamoxifen (40 mg/kg body weight) caused mosaic loss of *Prkar1a* floxed alleles but not immediate lethality (Supplementary Figure S2). Mice treated in this manner exhibited characteristic symptoms of cachexia, including delayed responsiveness, low physical activity, scruffy fur, pilo-erection and darkening of dorsal hair. These mice lost 15–20% of their body weight within a week of tamoxifen administration (Figure 4c) and therefore had to be

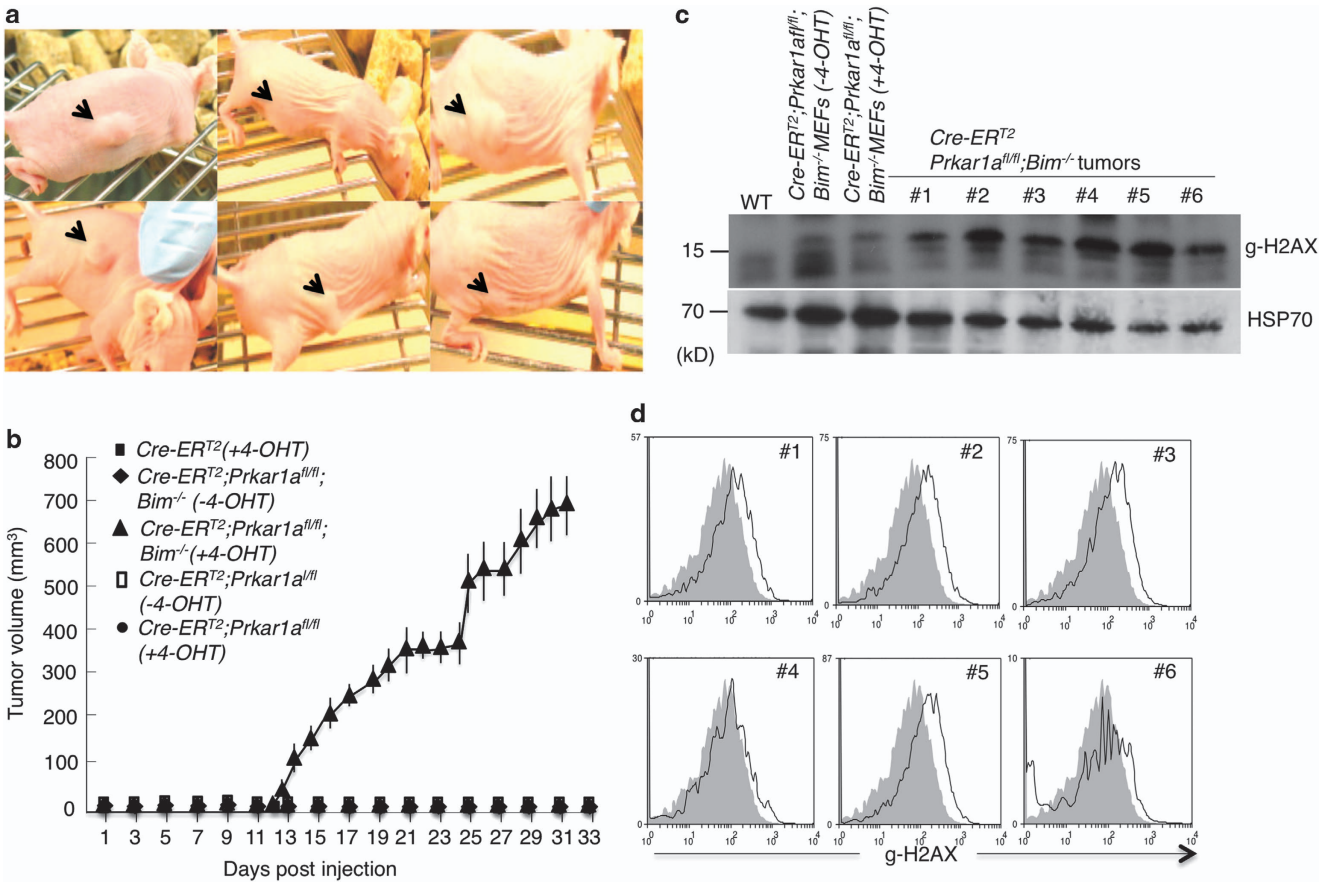

Figure 2 Combined deletion of *Bim* and *Prkar1a* promoted tumour growth by MEFs in immunodeficient BALB/c-nude mice with 100% penetrance. (**a**) *Bim*$^{-/-}$; *Prkar1a*$^{-/-}$ MEF grow as tumours in immunodeficient BALB/c-nude mice. Arrowheads indicate the site where MEFs were injected. (**b**) Summary of tumour growth by injected MEFs of the indicated genotypes. (**c** and **d**) Analysis of γ-H2AX levels in MEF-derived tumours as determined by western blotting or FACS. Error bars ± S.D., $n = 12$ for each genotype

culled for ethical reasons. Macrophage activation is often associated with the onset of cachexia.[25] We examined whether this was the case in these animals by using a quenched activity-based probe (LE28) against legumain, a lysosomal cysteine protease that is highly expressed in activated macrophages.[26] Tail vein injection of LE28 showed substantially increased legumain activity in *Prkar1a*-deleted mice compared with control animals, suggesting increased macrophage activation (Figure 5a). However, this activation was not intrinsic to macrophages as a result of *Prkar1a* deletion. The bone marrow-derived macrophages from *ROSA-CreER*^{T2};*Prkar1a*$^{fl/fl}$ mice treated with 4-OHT in culture failed to secrete any pro-inflammatory cytokines compared with the same macrophages treated with LPS (Supplementary Figure S3c). The legumain staining seen in the *ROSA-CreER*^{T2} control mouse (ventral view, Figure 5a) was a consequence of the probe being cleared by the bladder. It is noteworthy that the kidney has a high basal level of legumain activity. These results were further corroborated by imaging and western blot analysis of various tissues (Supplementary Figure S3b). The cachexia in the *Prkar1a*-deleted mice was also characterized by atrophy of *Tibialis anterior* and depletion of subscapular and epididymal fat deposits (Figure 5b). Consistent with increased lipolysis in cachexia,[27] we found increased phosphor-HSL (hormone-stimulated lipase) levels in adipose tissues and increased free triglycerides in the sera from the *Prkar1a*-deleted mice (Figures 5c and d). Upon *Prkar1a* deletion, all mice underwent rapid weight loss and muscle wasting. Loss of *Bim* did have a protective effect in several organs of these animals. For example, loss of *Bim* substantially reduced the splenic and thymic atrophy caused by induced loss of *Prkar1a* demonstrating that *Bim* is critical for the death of lymphoid cells elicited by elevated PKA signalling. However, loss of *Bim* did not afford substantial protection in other affected tissues, such as the heart and kidney. This indicates that other BH3-only proteins, probably PUMA, have a more important role (either alone or overlapping with BIM) in these organs (Figures 4b and c and Supplementary Figures S4a and b). Accordingly, western blot and qPCR analyses showed that *Puma* expression levels were substantially upregulated in the liver and spleen of tamoxifen-injected *ROSA-CreER*^{T2};*PRKAR1A*$^{fl/fl}$ mice (Supplementary Figures S4c and d). To further understand the role of PUMA in this apoptosis pathway, we generated bone marrow-derived factor-dependent myeloid cells (FDMs)[28] from

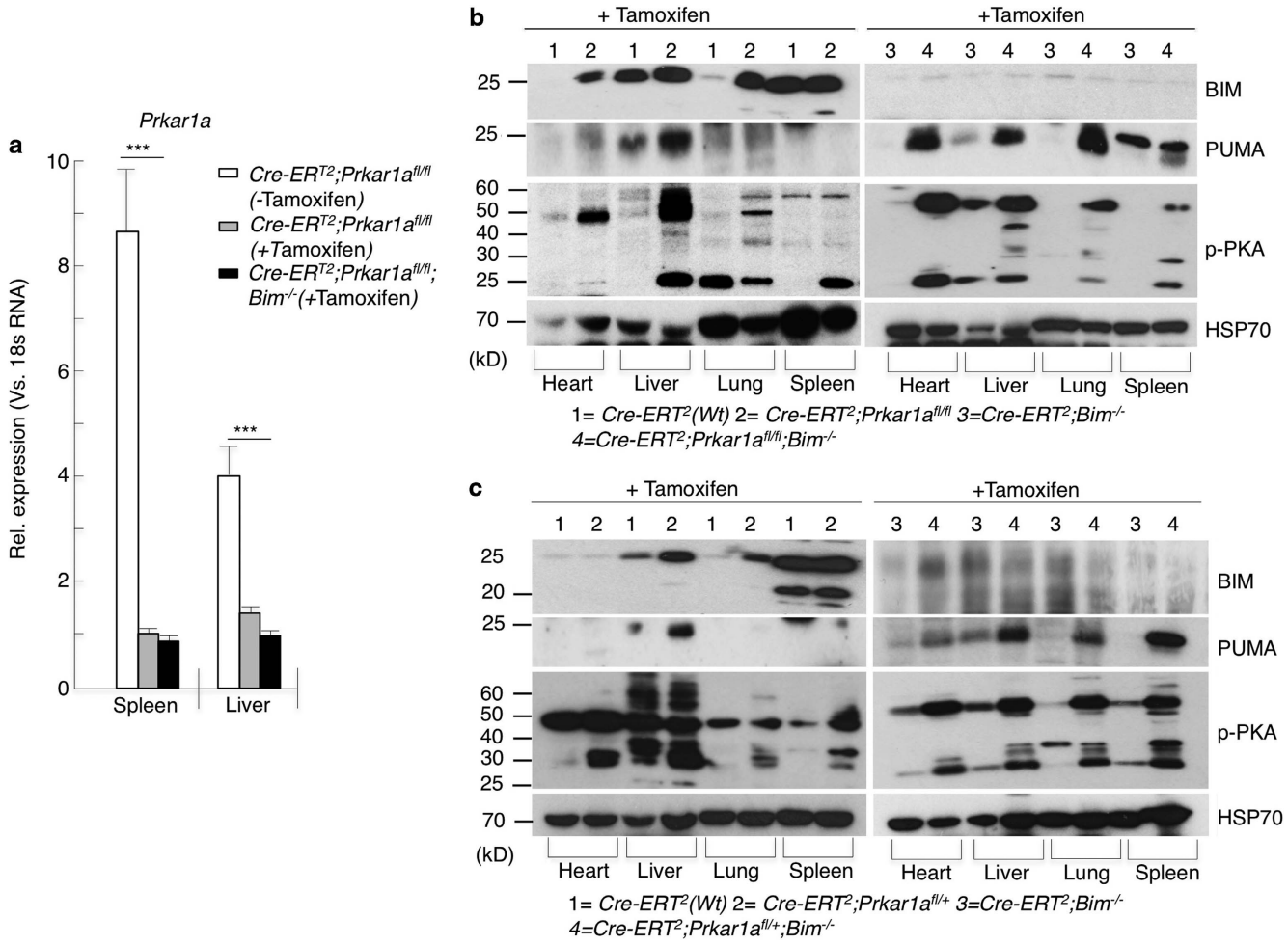

Figure 3 Inducible systemic deletion of *Prkar1a* caused an increase in *Bim* and *Puma* expression in several tissues. (**a**) Mice were injected subcutaneously (s.c.) with tamoxifen and 7 days later spleen and liver samples were analysed by qPCR and (**b** and **c**) western blot analyses for the expression of BIM and PUMA in various tissues of mice in different genotypes as indicated. Error bars ± S.E.M., $n=3$, two-tailed *t*-tests. ***$P<0.001$

ROSA-CreER^{T2};Prkar1a$^{fl/fl}$;Bim $^{-/-}$ mice. These cells were infected with lentiviruses expressing either *Puma*-specific shRNA or control shRNA (Supplementary Figure S5b, inset). Treating the parental cells or cells with control shRNA with 4-OHT led to a significant induction of caspase 3 activation and apoptosis at 72 h post treatment (Supplementary Figures S5a, b and c). However, this effect was significantly reduced in cells expressing *Puma*-specific shRNA confirming the role of PUMA in this apoptosis process.

Loss of one allele of Prkar1a does not enhance carcinogen-induced tumour. Patients with CNC (caused by Prkar1α deficiency) develop skin lesions, myxomas, collagenomas and fibromas.[2,29] Therefore, we examined whether *Prkar1a* deficiency could elicit benign, noninflammatory skin lesions. We investigated this by using a two-stage protocol, involving a single topical application of 7,12-dimethylbenz(a)anthracene (DMBA), which causes mutation of the Hras oncogene in keratinocytes with high frequency.[30] This was followed by repeated applications of 12-O-tetradecanoylphorbol-13-acetate (TPA), an inducer of cell proliferation that promotes the formation of papillomas.[31] Notably, activation of the H-Ras signalling pathway has been implicated in excessive cell proliferation caused by *Prkar1a* haploinsufficiency in human patients.[7,32] We used *ROSA-CreER^{T2};Prkar1a $^{fl/+}$* for this experiment because *ROSA-CreER^{T2};Prkar1a$^{fl/fl}$* injected with tamoxifen died within a week due to cachexia. *ROSA-CreER^{T2}*, *ROSA-CreER^{T2};Bim $^{-/-}$*, *ROSA-CreER^{T2};Prkar1a $^{fl/+}$* and *ROSA-CreER^{T2};Prkar1a $^{fl/+}$;Bim $^{-/-}$* mice ($n=6$ in each genotype) were injected with tamoxifen (40 mg/kg for three consecutive days) followed by a single topical application of DMBA. This was followed by weekly topical application of TPA and the mice were observed for a period of 30 weeks for skin lesions. As shown in Figure 6a, there was no significant difference between *ROSA-CreER^{T2}* (control), *ROSA-CreER^{T2};Bim $^{-/-}$* and *ROSA-CreER^{T2};Prkar1a$^{fl/+}$* mice with respect to the rate and incidence of skin tumour development. Contrary to expectations, tumour development was significantly ($P<0.001$) delayed in *ROSA-CreER^{T2};Prkar1a$^{fl/+}$;Bim $^{-/-}$* mice. *ROSA-CreER^{T2}; Prkar1a$^{fl/+}$;Bim $^{-/-}$* and *ROSA-CreER^{T2};Prkar1a$^{fl/fl}$;Bim $^{-/-}$* tissues (including heart, liver,

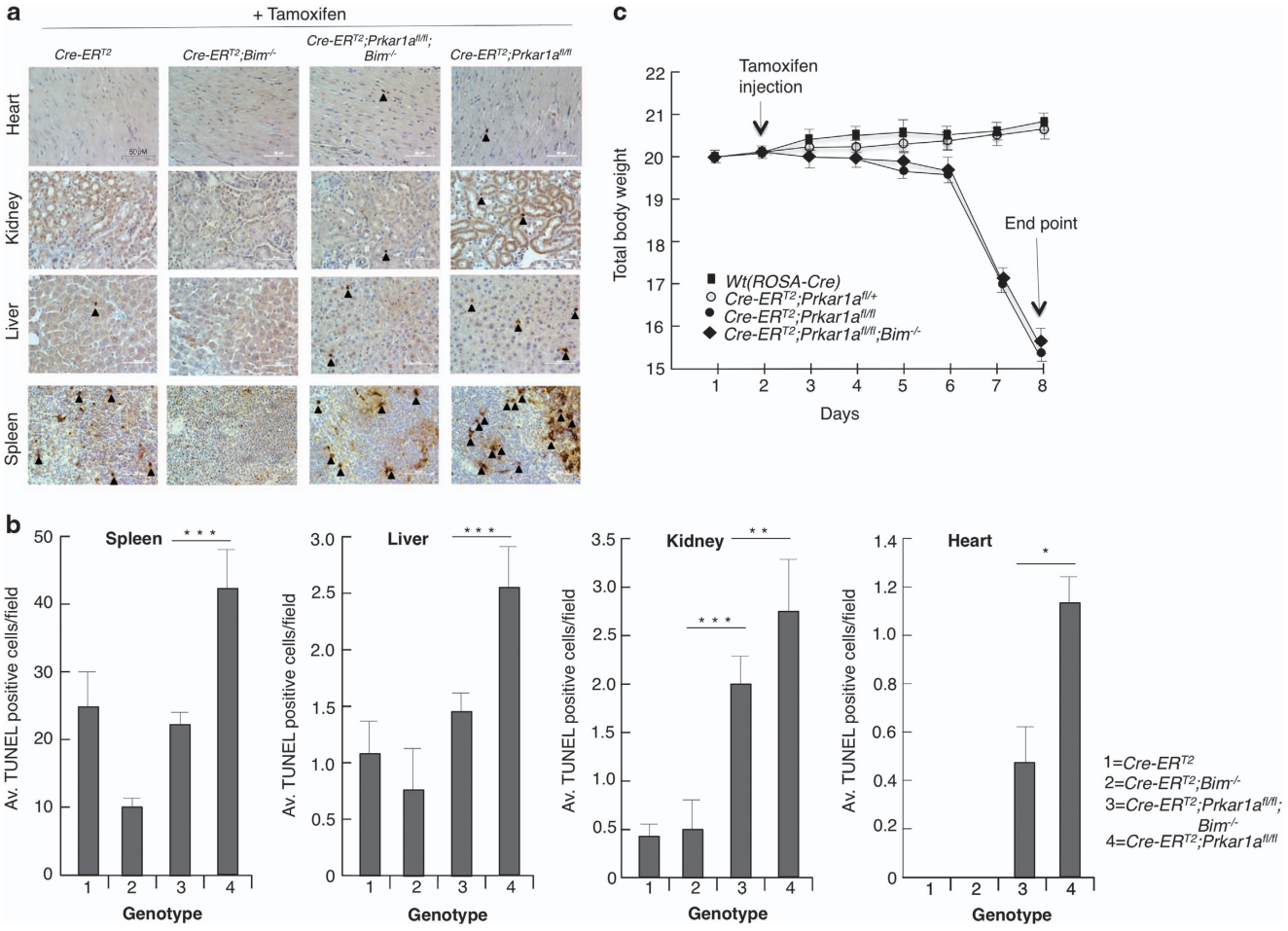

Figure 4 Induced deletion of *Prkar1a* caused apoptosis in several tissues. (**a**) Representative TUNEL staining of histological sections of the indicated organs from mice of the indicated genotypes 7 days after tamoxifen injection. Arrowheads indicate TUNEL-positive cells (**b**) Quantitation of TUNEL-positive cells in the indicated organs from the mice of the indicated genotypes. (**c**) *Prkar1a* gene deletion led to acute weight loss and death. Body weight measurement of mice of each genotype on the indicated days after injection with tamoxifen. Mice with 15% reduction in body weight had to be killed for ethical reasons ($n=6$; three males and three females for each genotype). Error bars ± S.D., *$P=0.0039$, **$P=0.37$, ***$P=0.000008$, ****$P=0.0043$

lung and spleen) had elevated levels of PUMA (Figure 3 and Supplementary Figure S4c and d). Consistent with this, western blot and mRNA analyses revealed that single-copy *Prkar1a* deletion led to a significant increase in *Puma* (and *Noxa* by RNA analysis) levels in skin in the absence of *Bim* (Figures 6b and c). These results confirm the role of proapoptotic proteins BIM and PUMA in *Prkar1a* deletion-mediated tumorigenesis.

Discussion

Although the symptoms of CNC are highly variable, endocrine hyperactivity and skin lesions are common and usually associated with deregulated PKA activity. This increased PKA activity is attributed to *Prkar1a* haploinsufficiency.[2] Various mouse models have been developed to study CNC disease. Constitutive homozygous deletion of *Prkar1a* from conception causes embryonic lethality. Hence, most studies on PRKAR1α function relied on Cre-based conditional deletion of floxed *Prkar1a* alleles. A compounding factor in these previous studies is the use of a constitutively active Cre recombinase, which was found to lead to global attenuation of PKA activity.[20] Other studies, such as osteocalcin-driven SV40 T-antigen expression in osteoclasts implicated *Prkar1a* as a tumour suppressor.[33] In contrast, another report identified *Prkar1a* as a weak tumour promoter,[9] and our previous work revealed that increased PKA activity can elicit apoptosis, consistent with the notion that PRKAR1α may promote tumorigenesis.[11,12,34] We therefore hypothesized that *Prkar1a* loss or haploinsufficiency on its own would not be sufficient to promote tumour development. Tumorigenesis does not result from a single oncogenic mutation but is driven by a series of oncogenic lesions, each conferring some growth advantage. In the context of tumorigenesis driven by deregulated PKA activity, overcoming apoptosis appears to be a crucial and limiting event, as increased PKA activity causes increased expression of proapoptotic BH3-only proteins, such as BIM and PUMA. We examined this hypothesis by crossing *Prkar1a* $^{fl/fl}$ mice with *Bim* $^{-/-}$ mice and deleting the '*floxed*' allele by using the conditional

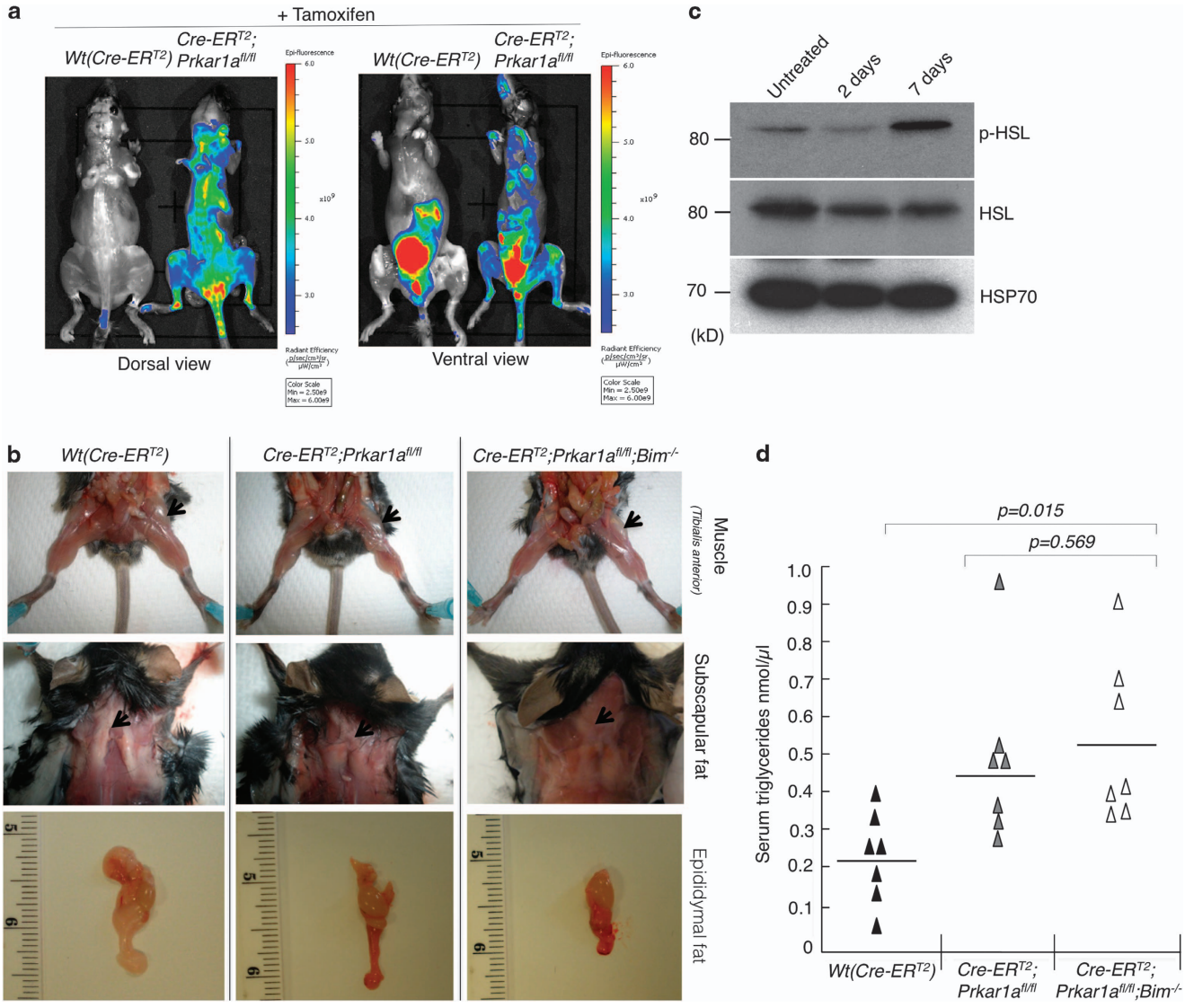

Figure 5 Induced systemic deletion of *Prkar1a* caused cachexia in mice. (**a**) Imaging of mice undergoing cachexia with legumain (LE28) staining. In the ventral view, the control (*ROSA-CreER*^{T2}) mouse also shows fluorescence in the bladder due to the clearance of the dye by the renal system. (**b**) Images of mice from the indicated genotypes showing loss of *Tibialis anterior* and subscapular and epididymal fat. (**c**) Western blot analysis of extracts of white adipose tissue from mice of the indicated genotypes 5 days after tamoxifen administration to determine the levels of activated hormone-induced lipase (p-HSL) and (**d**) serum triglyceride levels in mice measured ($n = 7$ for each genotype)

ROSA-Cre-ER^{T2} transgene (which, unlike several of the conventional Cre transgenes does not impact on PKA activity).[20]

Interestingly, loss of *Prkar1a* cooperated with loss of *Bim* in the transformation of MEFs in culture (clonogenic assay) and their ability to grow as tumours in immunodeficient mice. This can be explained by the observation that increased PKA (due to loss of *Prkar1a*) activity causes induction of several cell cycle promoters, such as cyclin D1, Cdk4 and E2F1,[9,10] but also augments expression of proapoptotic BH3-only proteins, most notably BIM. Thus, loss of *Bim* overcomes this restraint of neoplastic transformation that is activated as a safeguard when PKA activity is deregulated. This is reminiscent of the processes involved in tumorigenesis driven by deregulated c-MYC expression, whereby c-MYC enhances cellular metabolism, growth and proliferation but also predisposes cells to undergo apoptosis, particularly when growth conditions (e.g., availability of growth factors) are suboptimal.[35] Accordingly, deregulated c-MYC expression cooperates in tumorigenesis potently with defects in apoptosis, such as BCL-2 overexpression[36] or, similar to the situation with deregulated PKA activity, loss of *Bim*.[37]

Perhaps surprisingly, induced loss of *Prkar1a* within the whole mouse did not cause tumour development. First, TUNEL staining revealed that deletion of *Prkar1a* caused substantial apoptosis in several tissues. Constitutive loss of *Bim* could inhibit this apoptosis in the thymus and spleen. This is consistent with our previous finding that activation of PKA by β-AR agonists in fetal thymic organ cultures caused *Bim* induction and BIM-mediated apoptosis.[12] In the present study, loss of *Bim* had only limited impact on the induction of apoptosis in several non-hematopoietic tissues, including the

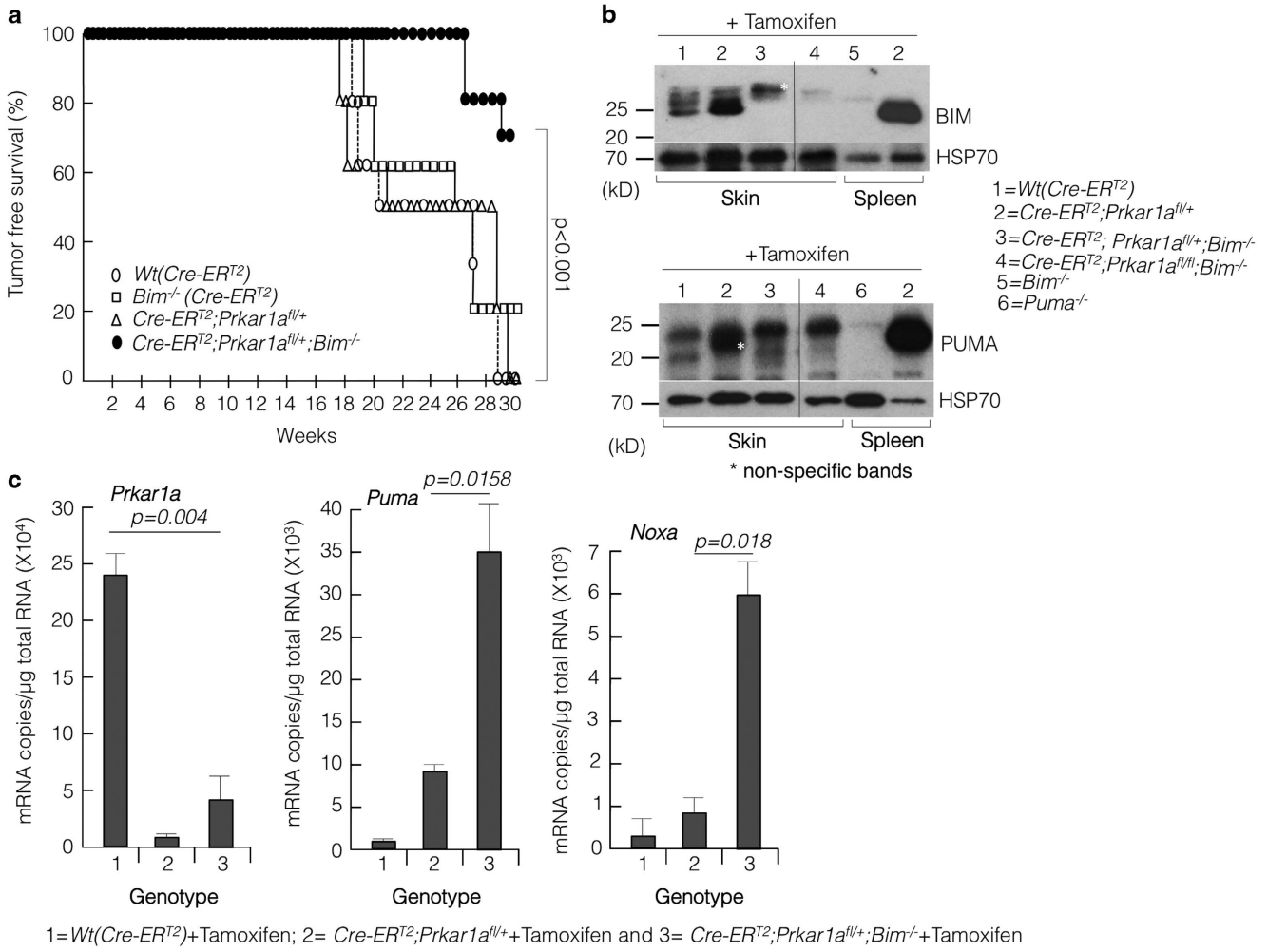

Figure 6 *Prkar1a* deletion did not promote carcinogen-induced tumorigenesis in mice. (**a**) Kaplan–Meier curve for tumour-free survival after the administration of DMBA and TPA. (**b**) Western blot analysis of skin tissues 5 days post administration of tamoxifen to determine the levels of BIM and PUMA. In each western blot, spleen extracts from wild-type, $Bim^{-/-}$ or $Puma^{-/-}$ mice were used to demonstrate antibody specificity. (**c**) RNA copy measurement from skin samples 5 days post tamoxifen treatment by digital droplet PCR. Error bars ± S.E.M., $n = 3$

heart, liver and kidneys. This indicates that other proapoptotic proteins, either on their own or in combination with *Bim*, might mediate this cell death. Notably, deletion of *Prkar1a* alone or together with constitutive loss of *Bim* resulted in substantial increases in *Puma* levels in these tissues. Hence, *Puma* might have a critical role in the cell death induced by *Prkar1a* deletion in these tissues. It is, however, also possible that other proapoptotic BH3-only proteins, such as NOXA, might have a role in this cell loss. The generation of mice with inducible deletion of *Prkar1a* that are deficient for *Puma*, *Bim* and *Noxa* may resolve some of these questions.

Interestingly, inducible deletion of *Prkar1a* caused acute weight loss, cachexia and death, and this could not be impeded by loss of *Bim*. Again, this might (at least in part) be due to increased expression of *Puma/Noxa*, thereby causing apoptosis of critical cell types in diverse tissues. The weight loss could be attributed to abnormally increased lipolysis, due to the fact that PKA activation causes phosphorylation and consequent activation of hormone-stimulated lipase (HSL).[38] This was evident from the loss of subscapular and epididymal fat deposits, serum triglyceride levels and in the level of p-HSL in the adipose tissues of *ROSA-CreER*$^{tg/tg}$*;Prkar1a*$^{fl/fl}$ and *ROSA-CreER*$^{tg/tg}$*;Prkar1a*$^{fl/fl}$*;BIM*$^{-/-}$ mice injected with tamoxifen (Figure 5). This lipolysis could occur irrespective of the *Bim* status. The increased macrophage activity revealed by legumain staining may reflect clearance of apoptotic cells.

In the chemically induced carcinogenesis model, constitutive loss of one *Prkar1a* allele did not accelerate the rate of tumour development. Curiously, constitutive loss of *Bim* substantially delayed the onset and severity of tumour development. Again, this might be attributed to increased *Puma* and *Noxa* expression as seen in the western blot and mRNA analysis of skin samples. We had previously reported that PKA activation leads to CREB-binding protein (CBP)-mediated induction of *Bim* (Lee *et al.*,[12]). CBP is also a transcriptional cofactor for p53[39] and hence might upregulate the expression of p53 target genes, such as *Puma* and *Noxa*. Therefore, it is conceivable that *Prkar1a* deletion leads to increased expression of *Puma* and *Noxa* in the skin tissues and that constitutive loss of *Bim* enables the cells to cope with increased levels of these proapoptotic BH3-only proteins. Notwithstanding the unexpected result, this underscores the

importance of BCL-2 family proteins in *Prkar1a* deletion-induced neoplasia and warrants further investigation.

The present study demonstrates unexpectedly that *Prkar1a* deletion activates a tumour-suppressive process by causing increased expression of proapoptotic BH3-only proteins. This goes against the currently prevailing opinion in the field that mutations in *Prkar1a* cause cancer. A possible explanation for this discrepancy might be that in the human tumours, the loss of function mutations in *Prkar1a* are accompanied by presently unknown mutations or epigenetic changes that counter the apoptosis that is driven by the excess PKA activation. Another question is why was no apoptosis observed in the previous studies of mouse models of Carney complex, where precise genetic mutations were introduced?[40] It might be relevant that these models all relied on the use of conventional Cre transgenic strains, which may have resulted in the dampening of PKA activity below the threshold needed for inducing apoptosis.

In conclusion, our studies reveal that inducible deletion of *Prkar1a* causes increased activation of PKA, but this does not promote tumorigenesis but rather triggers apoptosis in many tissues, severe weight loss and cachexia.

Materials and Methods

Animal experiments. All animal experiments were conducted according to guidelines of the La Trobe University Animal Ethics committee. The origins and genotyping protocols of the *Bim*$^{-/-}$,[41] *Puma*$^{-/-}$,[42] and *Prkar1a*$^{fl/fl}$ mice[43] have been described. ROSA-CreER^{T2} mice were a kind gift from Professor Tyler Jacks, MIT. The tumorigenicity of MEF lines was determined by measuring their ability to form tumours when injected subcutaneously into 6–8-week-old immunodeficient athymic nude mice on a BALB/c background. Each mouse was given an injection of 1×10^6 MEFs in 100 μl PBS using 25-gauge needles. Tumour size was measured daily along the longest axis (l) and at 90° (W) using digital callipers. Tumour volume was calculated with the formula ½($W^2 \times$ l). The time for tumour formation was defined as the time required for a tumour to reach a diameter of 5 mm. Mice had to be sacrificed for ethical reasons when the tumours had grown to a volume of 750 mm^3 or after 12 weeks of monitoring.

Antibodies and other reagents. BIM monoclonal antibodies (mAb 3C5) have been described.[44] HSP70 mAbs were a kind gift from Professor Robyn Anderson (Peter McCallum Cancer Institute, Melbourne). Antibodies to Gamma H2AX (Cat# ab-11174, Abcam, Cambridge, MA, USA), PRKAR1α (Cat# 610609, BD Biosciences, North Ryde, NSW, Australia); PKA substrate (Cat# 9621, Cell Signalling, Cambridge, MA, USA), PUMA (Cat#P4618, Sigma-Aldrich, St. Louis, MO, USA), HSL (Cat# 4107S, Cell Signalling); anti-legumain (Cat# AF2058, R&D Systems, Minneapolis, MN, USA) and phosphorylated HSL (Cat# 4126S, Cell Signalling) were purchased from the indicated vendors. 7,12-dimethylbenz[*a*]anthracene (DMBA) and TPA were purchased from Sigma (Castle Hill, NSW, Australia; Cat# D3254 and P1585, respectively).

Generation of FDMs and *Puma* shRNA knockdown. Factor-dependent myeloid (FDM) cells from *ROSA-CreER^{T2}, Prka1a$^{fl/fl}$, Bim*$^{-/-}$ mice were generated by immortalization with HoxB8 in the presence of high concentrations of IL-3 as described before.[28] These cells were infected with lentiviruses encoding mouse *Puma* shRNA or control shRNA on pLKO.1 vector backbone (Clone ID: TRCN0000009710, Open Biosystems, GE Healthcare, Rydalmere, NSW, Australia). The infected cells were selected on 0.4 μg/ml puromycin.

TUNEL staining of tissue sections. Tissues were fixed in HistoChoice tissue fixative (Cat# H2904-1L, Sigma) overnight. Fixed tissues were processed using Leica (Leica Biosystem, Melbourne, VIC, Australia) bench top tissue processor. After processing, the tissues were paraffin embedded and cut into 5 μm sections using Leica Microtome. Tissue sections were mounted on superfrost microscope slides and used for hematoxylin and eosin staining (H&E stain) or Terminal deoxynucleotidyl transferase dUTP nick end labelling (TUNEL). Before staining, the paraffin sections were de-waxed and treated with 20 mg/ml proteinase K. Endogenous peroxidase activity of tissues was blocked by treatment with 10% H_2O_2 in methanol. For each section 50 μl of TUNEL reaction mix was prepared as follows: Bio dUTP (0.3 nmol/ml, Cat# 1093070, Roche, Indianapolis, IN, USA), CoCl2 (25 mM), 5 $\times$ TdT buffer (Cat# M189A, Promega, Alexandria, NSW, Australia). TdT (25 U/ml, Cat# M187A, Promega) in a total volume of 50 μl. Sections were incubated in TUNEL reaction mix for 1 h at 37 °C (Cat# M187A, Promega). TUNEL reaction mix without terminal deoxynucleotide transferase (TdT from Promega, Cat# M187A) was used as a negative control for each section. After several washes in PBS, sections were incubated with ABC reagent (Vectastain Elite ABC Kit, Cat# PK-61000, Vector labs, Cambridgeshire, UK) for 30 min at R.T. Following several washes in PBS, the sections were incubated in DAB peroxidase substrate mixture for 5 min. The sections were washed in tap water, counterstained and mounted in DPX mounting medium (TCS Biosciences, Buckingham, UK) before observing under the microscope.

Assessing Legumain activity in mice and tissues. Age-matched mice were injected with LE28 (20 nmol in 20% DMSO/PBS, $\sim$2 mg/kg). An hour later, mice were humanely killed and the skin was removed. The mice were then imaged for Cy5 fluorescence using the IVIS Lumina system. Tissues were harvested, imaged *ex vivo*, and then sonicated in hypotonic lysis buffer (50 mM PIPES (pH 7.4), 10 mM KCl, 5 mM KCl_2, 2 mM EDTA, 4 mM DTT, and 1% NP-40). Supernatants were collected after centrifugation and total protein concentration was determined by BCA assay. Lysates were solubilized by adding 4 $\times$ sample buffer, and 100 μg protein was resolved by SDS-PAGE. The gel was then scanned using a Typhoon (GE Healthcare) flatbed laser scanner (excitation 633 nm/emission 670 nm). Proteins were then transferred to nitrocellulose membrane to blot for total legumain expression (R&D sheep anti-mouse legumain AF2058) and HSP70 for loading control.

Serum triglyceride analysis. Blood from mice was collected into K_2EDTA anti-coagulant containing tubes. The tubes were centrifuged at 1000 r.p.m. for 5 min to separate the plasma. Triglyceride levels in the plasma were measured using Triglyceride Quantification Kit (Cat# ab65336, Abcam) following manufacturer's instructions.

Gene expression analysis. Total RNA was isolated using TRIZOL (Cat#15596-026, Invitrogen, Carlsbad, CA, USA). Complementary DNA (cDNA) was synthesized from 2.5 μg of total RNA using the Superscript III RT-PCR system (Cat# 18080-051 Invitrogen). cDNA samples were tested in triplicate either on a Light cycler 480 Real-time PCR instrument (Roche) using Sybr Green master mix (Cat# 4367659, Life Technologies, Melbourne, VIC, Australia) or on a QX200 Droplet Digital System using EvaGreen ddPCR Supermix (Bio-Rad, Gladesville, NSW, Australia). Following primer pairs were used for each gene: *Bim* (F): 5′-GAGTTGTGACAAGTCAACACAAACC-3′; *Bim* (R): 5′-GAAGATAAAGCGTAACAGTTGTAAGATA-3′; *Nur77* (F): 5′-CCTGTTGCTAGAGTCTGCCTTC-3′; *Nur77* (R): 5′-CAATCCAATCACCAAAGCCACG-3′; *Puma* (F): 5′-ATGCCTGCCTCACCTTCATCT-3′*; Puma* (R): 5′-AGCACAGGATTCACAGTCTGGA-3′; *Noxa* (F): 5′-ACTGTGGTTCTGGCGCAGAT-3′*; Noxa* (R): 5′-TTGAGCACACTCGTCCTTCAA-3′; *Prkar1a* (F): 5′-ATGGCGTCTGGCAGTATGGCA-3′ *Prkar1a (R)* 5′-GATGCCGGTTTTCTGTAGACA-3′; *18s rRNA* (F): 5′-CCGCTCCCAAGATCCAACTA-3′ and *18s rRNA* (R): 5′-TTGGAGGGCAAGTCTGGTG-3′.

Statistical analysis. Paired, two-tailed Student's *t*-test was used to determine the statistical significance in all experiments except for the Kaplan–Meier survival analysis (Figure 6) where Person's χ^2 test was used.

Conflict of Interest

The authors declare no conflict of interest.

Acknowledgements. We thank Anissa Jabbour, Liam O'Connor, Liz Milla, Philippe Bouillet, Ann Lin and Claretta D'Souza for reagents and advice and the LARTF staff for the care and maintenance of mice. LG is supported by CRC-BT and HP is supported by ARC Future Fellowship (FT0990683) and by ARC project grant (DP110100417). CH is supported by an ARC Future Fellowship (FT0991464).

Author contributions

HP, LG designed the experiments. LG, NN, MD, JO, CH, LO, LE and HP performed the experiments and LG, HG, LO, LE, MB, PE, AS and HP analysed the data and HP prepared the manuscript.

1. Carney JA. Carney complex: the complex of myxomas, spotty pigmentation, endocrine overactivity, and schwannomas. *Semin Dermatol* 1995; **14**: 90–98.
2. Stratakis CA, Kirschner LS, Carney JA. Clinical and molecular features of the Carney complex: diagnostic criteria and recommendations for patient evaluation. *J Clin Endocrinol Metab* 2001; **86**: 4041–4046.
3. DeMarco L, Stratakis CA, Boson WL, Jakbovitz O, Carson E, Andrade LM *et al.* Sporadic cardiac myxomas and tumors from patients with Carney complex are not associated with activating mutations of the Gs alpha gene. *Hum Genet* 1996; **98**: 185–188.
4. Kirschner LS, Carney JA, Pack SD, Taymans SE, Giatzakis C, Cho YS *et al.* Mutations of the gene encoding the protein kinase A type I-alpha regulatory subunit in patients with the Carney complex. *Nat Genet* 2000; **26**: 89–92.
5. Groussin L, Kirschner LS, Vincent-Dejean C, Perlemoine K, Jullian E, Delemer B *et al.* Molecular analysis of the cyclic AMP-dependent protein kinase A (PKA) regulatory subunit 1A (PRKAR1A) gene in patients with Carney complex and primary pigmented nodular adrenocortical disease (PPNAD) reveals novel mutations and clues for pathophysiology: augmented PKA signaling is associated with adrenal tumorigenesis in PPNAD. *Am J Hum Genet* 2002; **71**: 1433–1442.
6. Casey M, Vaughan CJ, He J, Hatcher CJ, Winter JM, Weremowicz S *et al.* Mutations in the protein kinase A R1alpha regulatory subunit cause familial cardiac myxomas and Carney complex. *J Clin Invest* 2000; **106**: R31–R38.
7. Robinson-White A, Hundley TR, Shiferaw M, Bertherat J, Sandrini F, Stratakis CA. Protein kinase-A activity in PRKAR1A-mutant cells, and regulation of mitogen-activated protein kinases ERK1/2. *Hum Mol Genet* 2003; **12**: 1475–1484.
8. Frodin M, Peraldi P, Van Obberghen E. Cyclic AMP activates the mitogen-activated protein kinase cascade in PC12 cells. *J Biol Chem* 1994; **269**: 6207–6214.
9. Almeida MQ, Muchow M, Boikos S, Bauer AJ, Griffin KJ, Tsang KM *et al.* Mouse Prkar1a haploinsufficiency leads to an increase in tumors in the Trp53 $+/-$ or Rb1 $+/-$ backgrounds and chemically induced skin papillomas by dysregulation of the cell cycle and Wnt signaling. *Hum Mol Genet* 2010; **19**: 1387–1398.
10. Vossler MR, Yao H, York RD, Pan MG, Rim CS, Stork PJ. cAMP activates MAP kinase and Elk-1 through a B-Raf- and Rap1-dependent pathway. *Cell* 1997; **89**: 73–82.
11. Moujalled D, Weston R, Anderton H, Ninnis R, Goel P, Coley A *et al.* Cyclic-AMP-dependent protein kinase A regulates apoptosis by stabilizing the BH3-only protein Bim. *EMBO Rep* 2011; **12**: 77–83.
12. Lee YY, Moujalled D, Doerflinger M, Gangoda L, Weston R, Rahimi A *et al.* CREB-binding protein (CBP) regulates beta-adrenoceptor (beta-AR)-mediated apoptosis. *Cell Death Differ* 2013; **20**: 941–952.
13. Zhang L, Insel PA. The pro-apoptotic protein Bim is a convergence point for cAMP/protein kinase A- and glucocorticoid-promoted apoptosis of lymphoid cells. *J Biol Chem* 2004; **279**: 20858–20865.
14. Cho YJ, Kim JY, Jeong SW, Lee SB, Kim ON. Cyclic AMP induces activation of extracellular signal-regulated kinases in HL-60 cells: role in cAMP-induced differentiation. *Leuk Res* 2003; **27**: 51–56.
15. Deeble PD, Murphy DJ, Parsons SJ, Cox ME. Interleukin-6- and cyclic AMP-mediated signaling potentiates neuroendocrine differentiation of LNCaP prostate tumor cells. *Mol Cell Biol* 2001; **21**: 8471–8482.
16. Kim G, Choe Y, Park J, Cho S, Kim K. Activation of protein kinase A induces neuronal differentiation of HiB5 hippocampal progenitor cells. *Brain Res Mol Brain Res* 2002; **109**: 134–145.
17. Myklebust JH, Josefsen D, Blomhoff HK, Levy FO, Naderi S, Reed JC *et al.* Activation of the cAMP signaling pathway increases apoptosis in human B-precursor cells and is associated with downregulation of Mcl-1 expression. *J Cell Physiol* 1999; **180**: 71–80.
18. Xiao RP. Beta-adrenergic signaling in the heart: dual coupling of the beta2-adrenergic receptor to G(s) and G(i) proteins. *Sci STKE* 2001; **2001**: re15.
19. Weissinger EM, Oettrich K, Evans C, Genieser HG, Schwede F, Dangers M *et al.* Activation of protein kinase A (PKA) by 8-Cl-cAMP as a novel approach for antileukaemic therapy. *Br J Cancer* 2004; **91**: 186–192.
20. Gangoda L, Doerflinger M, Lee YY, Rahimi A, Etemadi N, Chau D *et al.* Cre transgene results in global attenuation of the cAMP/PKA pathway. *Cell Death Dis* 2012; **3**: e365.
21. Haigis KM, Kendall KR, Wang Y, Cheung A, Haigis MC, Glickman JN *et al.* Differential effects of oncogenic K-Ras and N-Ras on proliferation, differentiation and tumor progression in the colon. *Nat Genet* 2008; **40**: 600–608.
22. Sedelnikova OA, Horikawa I, Redon C, Nakamura A, Zimonjic DB, Popescu NC *et al.* Delayed kinetics of DNA double-strand break processing in normal and pathological aging. *Aging Cell* 2008; **7**: 89–100.
23. Podhorecka M, Skladanowski A, Bozko P. H2AX phosphorylation: its role in DNA Damage response and cancer therapy. *J Nucleic Acids* 2010; **2010,** pii: 920161.
24. Yin Z, Jones GN, Towns 2nd WH, Zhang X, Abel ED, Binkley PF *et al.* Heart-specific ablation of Prkar1a causes failure of heart development and myxomagenesis. *Circulation* 2008; **117**: 1414–1422.
25. Johns N, Stephens NA, Fearon KC. Muscle wasting in cancer. *Int J Biochem Cell Biol* 2013; **45**: 2215–2229.
26. Edgington LE, Verdoes M, Ortega A, Withana NP, Lee J, Syed S *et al.* Functional imaging of legumain in cancer using a new quenched activity-based probe. *J Am Chem Soc* 2013; **135**: 174–182.
27. Agustsson T, Ryden M, Hoffstedt J, van Harmelen V, Dicker A, Laurencikiene J *et al.* Mechanism of increased lipolysis in cancer cachexia. *Cancer Res* 2007; **67**: 5531–5537.
28. Jabbour AM, Daunt CP, Green BD, Vogel S, Gordon L, Lee RS *et al.* Myeloid progenitor cells lacking p53 exhibit delayed up-regulation of Puma and prolonged survival after cytokine deprivation. *Blood* 2010; **115**: 344–352.
29. Carney JA, Gordon H, Carpenter PC, Shenoy BV, Go VL. The complex of myxomas, spotty pigmentation, and endocrine overactivity. *Medicine (Baltimore)* 1985; **64**: 270–283.
30. Roop DR, Lowy DR, Tambourin PE, Strickland J, Harper JR, Balaschak M *et al.* An activated Harvey ras oncogene produces benign tumours on mouse epidermal tissue. *Nature* 1986; **323**: 822–824.
31. Hawley-Nelson P, Stanley JR, Schmidt J, Gullino M, Yuspa SH. The tumor promoter, 12-O-tetradecanoylphorbol-13-acetate accelerates keratinocyte differentiation and stimulates growth of an unidentified cell type in cultured human epidermis. *Exp Cell Res* 1982; **137**: 155–167.
32. Robinson-White AJ, Leitner WW, Aleem E, Kaldis P, Bossis I, Stratakis CA. PRKAR1A inactivation leads to increased proliferation and decreased apoptosis in human B lymphocytes. *Cancer Res* 2006; **66**: 10603–10612.
33. Molyneux SD, Di Grappa MA, Beristain AG, McKee TD, Wai DH, Paderova J *et al.* Prkar1a is an osteosarcoma tumor suppressor that defines a molecular subclass in mice. *J Clin Invest* 2010; **120**: 3310–3325.
34. Rahimi A, Lee YY, Abdella H, Doerflinger M, Gangoda L, Srivastava R *et al.* Role of p53 in cAMP/PKA pathway mediated apoptosis. *Apoptosis* 2013; **12**: 1492–1499.
35. Pelengaris S, Khan M, Evan G. c-MYC: more than just a matter of life and death. *Nat Rev Cancer* 2002; **2**: 764–776.
36. Strasser A, Harris AW, Bath ML, Cory S. Novel primitive lymphoid tumours induced in transgenic mice by cooperation between myc and bcl-2. *Nature* 1990; **348**: 331–333.
37. Egle A, Harris AW, Bouillet P, Cory S. Bim is a suppressor of Myc-induced mouse B cell leukemia. *Proc Natl Acad Sci USA* 2004; **101**: 6164–6169.
38. Djouder N, Tuerk RD, Suter M, Salvioni P, Thali RF, Scholz R *et al.* PKA phosphorylates and inactivates AMPKalpha to promote efficient lipolysis. *The EMBO J* 2010; **29**: 469–481.
39. Pasqualucci L, Dominguez-Sola D, Chiarenza A, Fabbri G, Grunn A, Trifonov V *et al.* Inactivating mutations of acetyltransferase genes in B-cell lymphoma. *Nature* 2011; **471**: 189–195.
40. Nadella KS, Jones GN, Trimboli A, Stratakis CA, Leone G, Kirschner LS. Targeted deletion of Prkar1a reveals a role for protein kinase A in mesenchymal-to-epithelial transition. *Cancer Res* 2008; **68**: 2671–2677.
41. Bouillet P, Metcalf D, Huang DC, Tarlinton DM, Kay TW, Kontgen F *et al.* Proapoptotic Bcl-2 relative Bim required for certain apoptotic responses, leukocyte homeostasis, and to preclude autoimmunity. *Science* 1999; **286**: 1735–1738.
42. Villunger A, Michalak EM, Coultas L, Mullauer F, Bock G, Ausserlechner MJ *et al.* p53- and drug-induced apoptotic responses mediated by BH3-only proteins puma and noxa. *Science* 2003; **302**: 1036–1038.
43. Pasqualucci L, Kitaura Y, Gu H, Dalla-Favera R. PKA-mediated phosphorylation regulates the function of activation-induced deaminase (AID) in B cells. *Proc Natl Acad Sci USA* 2006; **103**: 395–400.
44. O'Reilly LA, Kruse EA, Puthalakath H, Kelly PN, Kaufmann T, Huang DC *et al.* MEK/ERK-mediated phosphorylation of Bim is required to ensure survival of T and B lymphocytes during mitogenic stimulation. *J Immunol* 2009; **183**: 261–269.

Supplementary Information accompanies this paper on Cell Death and Differentiation website (http://www.nature.com/cdd)